

# SUPERSYMMETRIC CP PROBLEM WITHOUT FLAVOUR VIOLATION \* \*\*

JANUSZ ROSIEK

Institute of Theoretical Physics, Warsaw University  
Hoża 69, 00-681 Warszawa, Poland

*(Received October 26, 1999)*

In the unconstrained MSSM, we reanalyze the constraints on the phases of supersymmetric flavour conserving couplings that follow from the electron and neutron electric dipole moments. We find that the constraints become weak if at least one exchanged superpartner mass is  $> \mathcal{O}(1 \text{ TeV})$  or if we accept large cancellations among different contributions. However, such cancellations have no evident underlying symmetry principle. For light superpartners, models with small phases look like the easiest solution to the experimental EDM constraints. This conclusion becomes stronger the larger is the value of  $\tan \beta$ . We discuss also the dependence of  $\varepsilon_K$ ,  $\Delta m_B$  and  $b \rightarrow s\gamma$  decay on those phases. We show that even in the absence of genuinely supersymmetric sources of CP violation MSSM contributions may affect the determination of the Kobayashi-Maskawa phase  $\delta_{\text{KM}}$ .

PACS numbers: 11.30.Er, 12.60.Jv, 13.40.Er

## 1. Introduction

In the Minimal Supersymmetric Standard Model (MSSM) there are new potential sources of the CP non-conservation effects. One can distinguish two categories of such sources. One is independent of the physics of flavour non-conservation in the neutral current sector and the other is closely related to it. To the first category belong, in principle arbitrary, the phases of the parameters  $\mu$ , gaugino masses  $M_i$ , trilinear scalar couplings  $A_I$  and  $m_{12}^2$ . They can be present even if the sfermion sector is flavour conserving.

---

\* Presented at the XXIII International School of Theoretical Physics "Recent Developments in Theory of Fundamental Interactions", Ustroń, Poland, September 15–22, 1999.

\*\* Supported in part by the Polish Committee for Scientific Research under the grant number 2 P03B 030 14.

The other potential phases may appear in flavour off-diagonal sfermion mass matrix elements  $\Delta m_{ij}^2$  and in flavour off-diagonal LR mixing parameters  $A_{ij}$ . These potentially new sources of CP violation are, therefore, closely linked to the physics of flavour and, for instance, vanish in the limit of flavour diagonal (in the basis where quarks are diagonal) sfermion mass matrices. It is, therefore, quite likely that the two categories of the potential CP violation in the MSSM are controlled by different physical mechanisms. They should be clearly distinguished and discussed independently.

Experimental constraints on the “flavour-conserving” phases come mainly from the electric dipole moments (EDM) of electron [1] and neutron [2]:

$$\begin{aligned} E_e^{\text{exp}} &< 4.3 \cdot 10^{-27} e \cdot \text{cm}, \\ E_n^{\text{exp}} &< 6.3 \cdot 10^{-26} e \cdot \text{cm}. \end{aligned}$$

The common belief was that the constraints from the electron and neutron EDM are strong [3,4] and the new phases must be very small. More recent calculations performed in the framework of the minimal supergravity [5,6] and non-minimal models [7] indicated the possibility of cancellations between various phases and, therefore, of weaker limits on the phases in some non-negligible range of parameter space. However, the new detailed analysis of Ref. [8] shows that such cancellations are accidental (there is no underlying symmetry principle) and require strong fine-tuning between various phases.

The new flavour-conserving phases in the MSSM may appear in the following terms in the superpotential and in the soft breaking Lagrangian:

$$W_{\text{CP}} = \mu H^1 H^2. \quad (1)$$

$$\begin{aligned} \mathcal{L}_{\text{soft-CP}} = & \frac{1}{2} \left( M_3 \tilde{G}^a \tilde{G}^a + M_2 \tilde{W}^i \tilde{W}^i + M_1 \tilde{B} \tilde{B} \right) + m_{12}^2 H^1 H^2 \\ & + Y_e A_e H^1 L E^c + Y_d A_d H^1 Q D^c + Y_u A_u H^2 Q U^c + \text{H.c.} \end{aligned} \quad (2)$$

We define phases as:

$$e^{i\phi_\mu} = \frac{\mu}{|\mu|} \quad e^{i\phi_i} = \frac{M_i}{|M_i|} \quad e^{i\phi_{A_I}} = \frac{A_I}{|A_I|} \quad e^{i\phi_H} = \frac{m_{12}^2}{|m_{12}^2|}. \quad (3)$$

Phases alone are not physical. In the absence of terms (1),(2) the MSSM Lagrangian has two global U(1) symmetries, an  $R$  symmetry and the Peccei-Quinn symmetry [9]. Terms (1),(2) may be treated as spurions breaking those symmetries, with appropriate charge assignments. Physical observables depend only on the phases of parameter combinations neutral under both U(1)’s transformation:

$$M_i \mu (m_{12}^2)^* \quad A_I \mu (m_{12}^2)^* \quad A_I^* M_i. \quad (4)$$

Not all of them are independent. The two  $U(1)$  symmetries may be used to get rid of two phases. The common choice is to keep  $m_{12}^2$  real in order to have real tree level Higgs field VEV's and  $\tan\beta$ . The second re-phasing may be used *e.g.* to make one of the gaugino mass terms real.

In Section 2 we discuss in detail the electron EDM - the magnitude of various contributions to the electron EDM and the pattern of possible cancellations. In Section 3 we analyze the neutron EDM with similar conclusions. In Section 4 we discuss the role of the  $\mu$  phase in the  $\varepsilon_K$  measurement and in the  $b \rightarrow s\gamma$  decay. In Section 5, we consider supersymmetric contributions to the CP violating processes assuming no new supersymmetric phases and discuss the influence of new MSSM contributions on predictions for the Kobayashi-Maskawa (KM) phase determination.

## 2. Electric dipole moment of the electron

### 2.1. Mass eigenstate vs. mass insertion calculation

The electric dipole moments of leptons and quarks, defined as the coefficient  $E$  of the operator

$$\mathcal{L}_E = -\frac{i}{2}E\bar{\psi}\sigma_{\mu\nu}\gamma_5\psi F^{\mu\nu}, \quad (5)$$

can be generated in the MSSM already at 1-loop level, assuming that supersymmetric parameters are complex.

In the mass eigenstate basis for all particles, two diagrams contribute to the electron EDM (see Fig. 1). The result for the lepton electric dipole moment reads (summation over all charginos, neutralinos, sleptons and sneutrinos in the loops is understood):

$$\begin{aligned} E_l^I &= \frac{em_l^I}{8\pi^2} \sum_{j=1}^2 \sum_{K=1}^3 m_{C_j} \text{Im} \left( (V_{l\bar{\nu}C})_L^{IKj} (V_{l\bar{\nu}C})_R^{IKj\star} \right) C_{11}(m_{C_j}^2, m_{\bar{\nu}_K}^2) \\ &- \frac{em_l^I}{16\pi^2} \sum_{j=1}^4 \sum_{k=1}^6 m_{N_j} \text{Im} \left( (V_{l\tilde{L}N})_L^{Ikj} (V_{l\tilde{L}N})_R^{Ikj\star} \right) C_{12}(m_{\tilde{L}_k}^2, m_{N_j}^2), \quad (6) \end{aligned}$$

where  $(V_{l\bar{\nu}C})_L$ ,  $(V_{l\bar{\nu}C})_R$ ,  $(V_{l\tilde{L}N})_L$ ,  $(V_{l\tilde{L}N})_R$  are, respectively, the left- and right- electron-sneutrino-chargino and electron-selectron-neutralino vertices and  $C_{11}$ ,  $C_{12}$  are the loop integrals (explicit form of the vertices and integrals can be found in [8, 10]). Eq. (6) is completely general, but as we discussed already in the Introduction, in the rest of this paper we assume no flavour mixing in the slepton sector. Hence, in the formulae below we skip the slepton flavour indices.

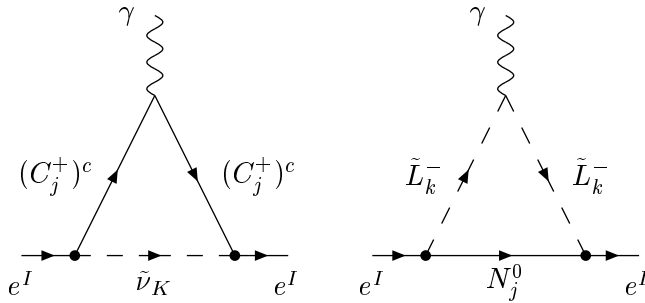


Fig. 1. Diagrams contributing to lepton EDM

We present now the calculation of the electron EDM in the mass insertion approximation, for easier understanding of cancellations of various contributions. We use the “generalized mass insertion approximation”, *i.e.* we treat as mass insertions both the L-R mixing terms in the squark mass mixing matrices and the off-diagonal terms in the chargino and neutralino mass matrices (see [8] for more details). Therefore we assume that the diagonal entries in the latter:  $|\mu|$ ,  $|M_{1,2}|$  are sufficiently larger than the off-diagonal entries, which are of the order of  $M_Z$ .

There are four diagrams with wino and charged Higgsino exchange, shown in Fig. 2.

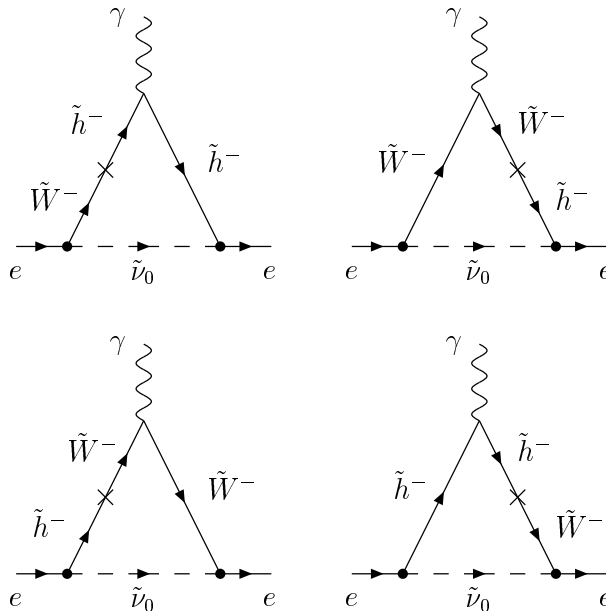


Fig. 2. Chargino contribution to lepton EDM in mass insertion expansion.

Their contribution to the electron EDM is ( $E_e \equiv E_l^1$ ):

$$(E_e)_C = \frac{2eg^2m_e}{(4\pi)^2} \text{Im}(M_2\mu) \tan\beta \frac{C_{11}(|\mu|^2, m_{\tilde{\nu}}^2) - C_{11}(|M_2|^2, m_{\tilde{\nu}}^2)}{|\mu|^2 - |M_2|^2}. \quad (7)$$

Neutral wino, bino and neutral Higgsino contributions can be split into two classes: with mass insertion on the fermion or on the sfermion line. Contribution of diagrams belonging to the first class has a structure very similar to that given by Eq. (7):

$$\begin{aligned} (E_e)_{Nf} = & -\frac{eg^2m_e}{2(4\pi)^2} \text{Im}(M_2\mu) \tan\beta \frac{C_{12}(m_E^2, |\mu|^2) - C_{12}(m_E^2, |M_2|^2)}{|\mu|^2 - |M_2|^2} \\ & + \frac{eg'^2m_e}{2(4\pi)^2} \text{Im}(M_1\mu) \tan\beta \frac{C_{12}(m_E^2, |\mu|^2) - C_{12}(m_E^2, |M_1|^2)}{|\mu|^2 - |M_1|^2} \\ & - \frac{eg'^2m_e}{(4\pi)^2} \text{Im}(M_1\mu) \tan\beta \frac{C_{12}(m_{E^c}^2, |\mu|^2) - C_{12}(m_{E^c}^2, |M_1|^2)}{|\mu|^2 - |M_1|^2}, \quad (8) \end{aligned}$$

where  $m_E$ ,  $m_{E^c}$  and  $m_{\tilde{\nu}}$  are the masses of left- and right- selectron and electron sneutrino, respectively. Between diagrams with mass insertions on the selectron line, only the two with bino line in the loop give sizeable contributions. The result is:

$$\begin{aligned} (E_e)_{Ns} = & \frac{eg'^2m_e}{(4\pi)^2} \text{Im}[M_1(\mu \tan\beta + A_e^*)] \\ & \times \frac{C_{12}(m_E^2, |M_1|^2) - C_{12}(m_{E^c}^2, |M_1|^2)}{m_E^2 - m_{E^c}^2}. \quad (9) \end{aligned}$$

Eqs. (7)–(9) have a simple structure: they are linear in the invariants (4), with coefficients that are functions of the real mass parameters. Thus, the possibility of cancellations depends primarily on the relative amplitudes and signs of those coefficients. An immediate conclusion following from (7)–(9) is that limits on the  $M_i\mu$  phases are inversely proportional to  $\tan\beta$ . Therefore, we discuss limits on  $\sin\phi_\mu \tan\beta$  rather than on the  $\mu$  phase itself.

The approximate formulae (7)–(9) work very well already for relatively small  $|\mu|$ ,  $|M_1|$  and  $|M_2|$  values, not much above the  $M_Z$  scale (see Fig. 3). The accuracy of the mass insertion expansion may become reasonable already for  $|\mu| \geq 150$  GeV and becomes very good for  $|\mu| \geq 200 - 250$  GeV.

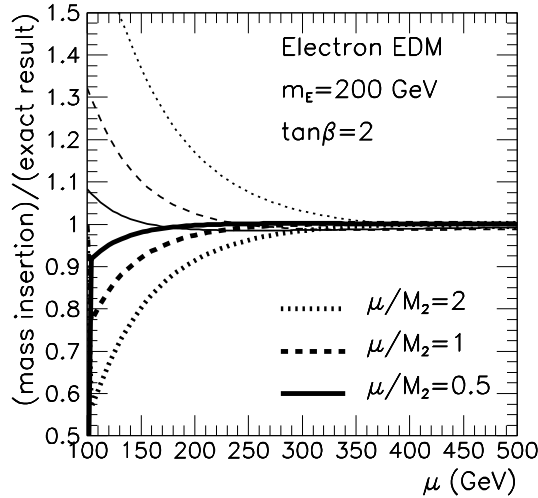


Fig. 3. Ratio of the electron EDM calculated in the mass insertion approximation to the exact 1-loop result. Thinner lines:  $\phi_\mu = 0$ , thicker lines:  $\phi_A = 0$ .

## 2.2. Limits on $\mu$ and $A_e$ phases

It is useful to consider two classes of models: one with  $M_1/\alpha_1 = M_2/\alpha_2 = M_3/\alpha_3$  for gaugino masses, that is universal gaugino masses at the GUT scale (the universal phase can be set to zero by convention), and the other with non-universal gaugino masses and arbitrary relative phase between  $M_1$  and  $M_2$ . In the universal case we choose  $\mu$  and  $A_e$  phases as the independent ones, in the second case the  $M_1, M_2$  phases are the additional free parameters. In all figures presented in this Section we assume the GUT-related gaugino masses and equal left and right slepton mass parameters,  $M_L = M_E$ , so that the physical masses of the left and right selectron differ by D-terms only. In addition, in the text we discuss possible effects of departure from those assumptions.

We shall begin our discussion by presenting the magnitude of each contribution (7), (8) and of the  $\mu$  and  $A_e$  terms in Eq. (9), separately. A sample of results is shown in Fig. 4. We identify there the parameter region where at least one of the terms is such that for  $\sin \phi_\mu \tan \beta$  fixed at some assumed value, its contribution to  $E_e$  is larger than  $E_e^{\text{exp}}$ . Barring potential cancellations, the fixed value of  $\sin \phi_\mu \tan \beta$  is then the limit on this phase in the identified parameter region. In the left (right) plot of Fig. 4 we show the regions of masses (below the plotted surface) where the limits on  $|\sin \phi_\mu| \tan \beta$  are stronger than 0.2 (0.05), respectively. The regions below the plotted surfaces are the regions of interest for potential cancellations. We observe, however, that even without cancellations, there are interest-

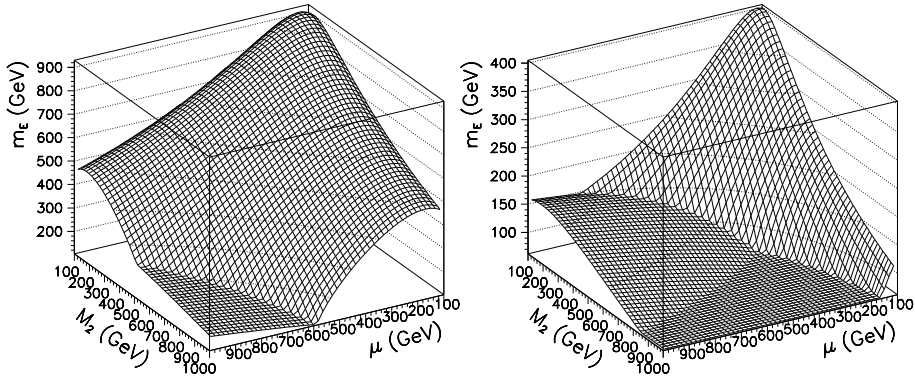


Fig. 4. Regions (below the dark surface) for which generic limits on  $|\sin \phi_\mu| \tan \beta$  are stronger then, respectively, 0.2 (left plot) and 0.05 (right plot).

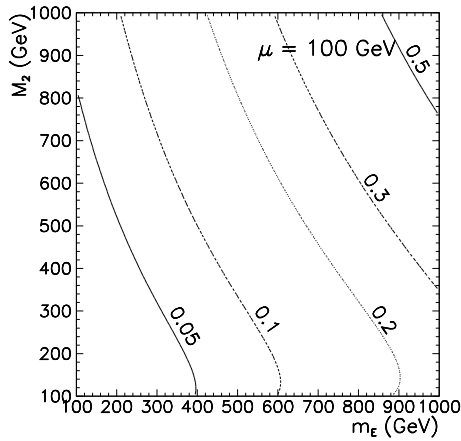


Fig. 5. Limits on  $|\sin \phi_\mu| \tan \beta$  given by the electron EDM measurements.  $\sin \phi_{A_e} = 0$  assumed.

ing regions of small  $|\mu|$  and  $|M_2|$  and  $m_E > \mathcal{O}(1 \text{ TeV})$  or small  $m_E$  and  $|\mu| \sim |M_2| > \mathcal{O}(500 \text{ TeV})$  where the phase of  $\mu$  is weakly constrained. One should also note that for very large  $|\mu|$  and the other masses fixed the limits on the  $\mu$  phase get stronger again. This is due to the term (9), which does not decouple for large  $|\mu|$ .

In Fig. 5 we show again the limits on  $\mu$  phase (given now by the sum of all terms (7)–(9), not by the largest of them like in Fig. 4), this time as a two-dimensional plot in the  $(m_E, |M_2|)$  plane, assuming  $\phi_{A_e} = 0$ . In Fig. 6 we show similar limits on the  $A_e$  phase on  $(m_E, |M_1|)$  plane, assuming  $\phi_\mu = 0$ . The limits on the  $A_e$  parameter phase are significantly weaker and decrease more quickly with increasing particle masses.

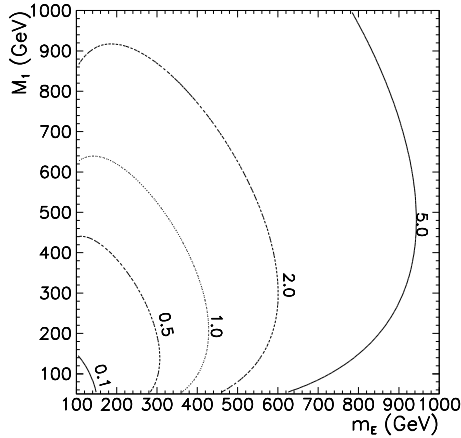


Fig. 6. Limits on  $|A_e/m_E \sin \phi_{A_e}|$  given by the electron EDM measurements ( $|\mu| = 200$  GeV and  $\sin \phi_\mu = 0$ ).

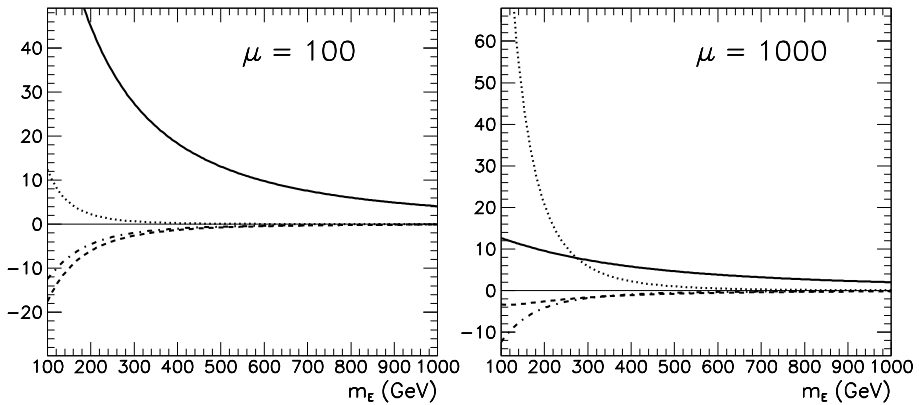


Fig. 7. Relative signs and amplitudes of various contributions to the electron EDM, normalized to (divided by) the experimental limit. Solid, dashed, dotted lines: coefficients of  $\sin \phi_\mu \tan \beta$  given by chargino (Eq. (7)) and neutralino contributions (Eqs. (8) and (9)) respectively. Dotted-dashed line: coefficient of  $|A_e \sin \phi_{A_e}|/m_E$ .

The magnitude and signs of individual contributions as a function of  $m_E$  are illustrated in Fig. 7. We plot there the coefficients of  $\mu$  and  $A_e$  phases obtained from the exact 1-loop result and normalized by dividing them by the experimental limit on the electron EDM. Their shape depends mostly on the  $m_E/|\mu|$  ratio, much less on the  $|\mu/M_2|$  ratio and scales like  $1/m_E^2$ . We see that either the chargino contribution to the term proportional to the  $\mu$  phase dominates (for small  $|\mu|$ ), or, if they become comparable (possible

only for larger values of  $|\mu| > 700$  GeV), the chargino and the dominant neutralino contribution, given by Eq. (9), to the  $\mu$  phase coefficient are of the same sign. Thus, the full coefficient of the  $\mu$  phase cannot vanish and the only possible cancellations are between the  $A_e$  and  $\mu$  phases.

Since the  $A_e$  phase coefficient is in the interesting region much smaller such cancellations always require large  $A_e$  in the selectron sector,  $A_e/m_E \gg 1$ . This is shown in Fig. 8, where we assume “maximal” CP violation  $\phi_\mu = \phi_{A_e} = \pi/2$ .

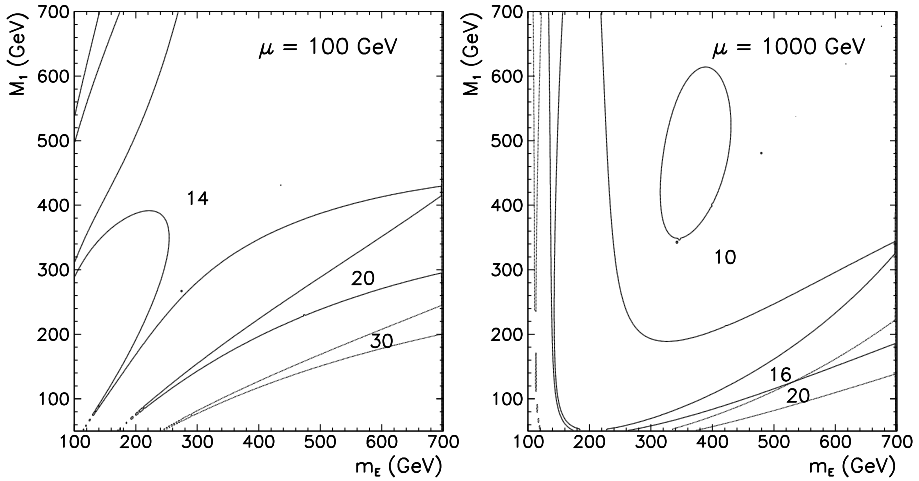


Fig. 8. Regions of  $m_E - M_1$  plane allowed by the electron EDM measurement assuming  $\phi_\mu = \phi_{A_e} = \pi/2$  and some values of  $A_e/m_E$  (marked on the plots).

Better understanding of the  $\mu$ - $A_e$  cancellation can be achieved after some approximations. For supersymmetric fermions significantly lighter than sleptons, chargino exchanges dominate, whereas in the opposite limit the biggest contribution is given by the diagrams with bino exchanges. Eqs. (7)–(9) can be greatly simplified in both cases, giving for degenerate slepton masses  $m_E \approx m_{E^c} \approx m_{\tilde{\nu}}$ :

1)  $|M_{1,2}|, |\mu| \ll m_E$

$$E_e \approx \frac{eg^2 m_e}{(4\pi)^2} \frac{\text{Im}(M_2 \mu) \tan \beta}{m_E^2 (|\mu|^2 - |M_2|^2)} \log \frac{|\mu|^2}{|M_2|^2} + \frac{eg'^2 m_e}{2(4\pi)^2} \frac{\text{Im}(M_1 A_e^*)}{m_E^4}; \quad (10)$$

2)  $|M_{1,2}|, |\mu| \gg m_E$

$$E_e \approx \frac{eg^2 m_e}{4(4\pi)^2} \frac{\text{Im}(M_2 \mu) \tan \beta}{|\mu|^2 |M_2|^2} - \frac{eg'^2 m_e}{4(4\pi)^2} \frac{\text{Im}(M_1 \mu) \tan \beta}{|\mu|^2 |M_1|^2} - \frac{eg'^2 m_e}{2(4\pi)^2} \frac{\text{Im}[M_1 (\mu \tan \beta + A_e^*)]}{|M_1|^4} \left( 5 + 2 \log \frac{m_E^2}{|M_1|^2} \right). \quad (11)$$

The behaviour of the lepton EDM is different in both limits. For heavy sleptons,  $|M_{1,2}|, |\mu| \ll m_E$  the coefficient of the  $\mu$  phase decreases with the increasing slepton mass as  $1/m_E^2$ . The coefficient of the  $A_e$  phase decreases faster, as  $1/m_E^4$ . Therefore, in this limit the exact cancellation between  $A_e$  and  $\mu$  phases requires large  $A_e$  value, growing with increasing  $m_E$ . However, because all contributions simultaneously decrease with increasing  $m_E$ , partial cancellation between  $\mu$  and  $A_e$  phase is already sufficient to push the electron EDM below the experimental limits, what may be observed in Fig. 8 as a widening of the allowed regions for large  $m_E$ .

For sufficiently small slepton masses the full cancellation between  $\mu$  and  $A_e$  terms occurs approximately for

$$\sin \phi_{A_e} |A_e| = \sin \phi_\mu |\mu| \tan \beta \left( 1 + \frac{|M_1|^2}{|\mu|^2} \frac{3}{5 + 2 \log(m_E^2/|M_1|^2)} \right). \quad (12)$$

Since this result is valid for  $|\mu|, |M_1|, |M_2| \gg m_E$  we see that for comparable  $\phi_\mu$  and  $\phi_{A_e}$  the cancellation is again possible only for large  $A_e/m_E \gg 1$ . For large  $|\mu| \gg |M_1|$ , when one can neglect the second term in the parenthesis in Eq. (12), the  $A_e$  giving maximal cancellation is almost independent of  $|M_1|$ , what can be observed in the right plot of Fig. 8. The allowed regions also widen with increasing  $|M_1|$ , but slower then for large  $m_E$  because the  $\mu$  and  $A_e$  phases are in this case suppressed by lower powers of  $|M_1|$ :  $1/|M_1|$  and  $1/|M_1|^3$  respectively, instead of  $1/m_E^2$  and  $1/m_E^4$ .

In the most interesting region of light SUSY masses, where the limits on phases are strongest, the cancellation between (fixed)  $\mu$  and  $A_e$  phases may occur only for very precisely correlated mass parameters, *i.e.* it requires strong fine tuning between  $|\mu|$ ,  $|M_{1,2}|$  and  $|A_e|$ . Analogously, for fixed light mass parameters one needs strong fine tuning of the order of  $\mathcal{O}(10^{-2})$  between the phases.

We shall discuss now the general case, with non-universal gaugino masses. The results for the magnitude of individual terms remain qualitatively similar to those shown in Fig. 4. The region of strong constraints on the  $\mu$  phase shrinks in  $m_E$  with increasing  $M_1$ . The magnitude of individual contributions as a function of  $m_E$  has very similar behaviour as in the universal case – again, for small  $|\mu|$  chargino contribution dominates for all values of  $|M_1|$  and  $|M_2|$ . The only possible cancellations for this  $|\mu|$  range are between  $\mu$  and  $A_e$  phases. For larger values of  $|\mu| > 700$  GeV the magnitude of individual terms may become comparable. With arbitrary relative phase of  $M_1$  and  $M_2$  it is possible to cancel the terms proportional to the  $\mu$  phase. To study this possibility it is more convenient to consider the contributions proportional to  $\text{Im}(\mu M_1)$  and  $\text{Im}(\mu M_2)$ . They are comparable for  $m_E/|\mu| \sim 1/5 - 1/3$ , depending on  $|M_1/M_2|$  ratio. It is clear that choosing  $\phi_1$  and  $\phi_2$  phases such that  $\sin(\phi_\mu + \phi_2)$  and  $\sin(\phi_\mu + \phi_1)$  have opposite signs, *e.g.*  $\phi_1 - \phi_2 \sim \pi$ , would give cancellation at these points.

### 3. EDM of the neutron

#### 3.1. Formulae for the neutron EDM

The structure of the neutron EDM is more complicated than in the electron case. It can be approximately calculated as the sum of the electric dipole moments of the constituent  $d$  and  $u$  quarks plus additional contributions coming from the chromoelectric dipole moments of quarks and gluons. The chromoelectric dipole moment (CDM)  $C_q$  of a quark is defined as:

$$\mathcal{L}_C = -\frac{i}{2}C_q\bar{q}\sigma_{\mu\nu}\gamma_5 T^a q G^{\mu\nu a}. \quad (13)$$

The gluonic CDM  $C_g$  is defined as:

$$\mathcal{L}_g = -\frac{1}{6}C_g f_{abc} G_{\mu\rho}^a G_{\nu}^{b\rho} G_{\lambda\sigma}^c \varepsilon^{\mu\nu\lambda\sigma}. \quad (14)$$

Exact calculation of the neutron EDM requires the full knowledge of its wave function. We use the “naive” chiral quark model approximation [12], which gives the following expression:

$$E_n = \frac{\eta_e}{3}(4E_d - E_u) + \frac{e\eta_c}{4\pi}(4C_d - C_u) + \frac{e\eta_g A_X}{4\pi}C_g, \quad (15)$$

where  $\eta_i$  and  $A_X$  are the QCD correction factors and chiral symmetry breaking scale:  $\eta_e \approx 1.53$ ,  $\eta_c \approx \eta_g \approx 3.4$  [13],  $A_X = 1.19$  GeV [12]. For the light quark masses we use  $m_d(A_X) = 10$  MeV,  $m_u(A_X) = 7$  MeV [14].

Eq. (15) contains sizeable theoretical uncertainties due to non-perturbative strong interactions. However, as we show in the next section, for most parameter choices  $E_d$  alone gives the leading contribution to the neutron EDM. Therefore, one may hope that those uncertainties affect mainly the overall normalization of the neutron EDM<sup>1</sup>. They do not affect significantly the possible cancellations between the phases (or in their coefficients), as long as such cancellations must occur predominantly inside the  $E_d$ . At present the limits on the phases given by the electron EDM are more precise and better established.

It was recently pointed out [15] that 2-loop contributions to the neutron EDM may be numerically significant, especially for large  $\tan\beta$  regime. Unlike most of the terms in Eq. (15), they depend mainly on the masses and mixing parameters of the third generation of squarks. Therefore, they are

---

<sup>1</sup> Any theoretical calculation of the overall normalization of the neutron EDM should be considered as a qualitative one - QCD correction may even change the sign of the factor multiplying  $E_d$  (see discussion in [8]).

especially important in the case of the third generation of squarks significantly lighter than the first two generation, so that the 1-loop contributions are suppressed. We do not include such corrections in the present analysis.

The explicit exact and mass insertion formulae for the up- and down quark electric and chromoelectric dipole moments, the gluonic chromoelectric dipole moment are given in Ref. [8].

### 3.2. Limits on phases

The neutron EDM depends on more phases than the electron EDM. All electric and chromoelectric dipole moments depend on the common  $\mu$  phase, but some of them are proportional to  $\mu \tan \beta$  and others to  $\mu \cot \beta$ , hence the limit on  $\mu$  phase does not scale simply like  $1/\tan \beta$ . In addition, the quark moments depend on the phases of the two LR mixing parameters of the first generation of squarks,  $A_d$  and  $A_u$ . The gluonic CDM depends mainly on the parameters of the 3rd generation of squarks,  $m_T$  and  $A_t$ . In practice, the analysis of the dependence of the neutron EDM on SUSY parameters appears less complicated than suggested by the above list, as some of the parameters have small numerical importance.

The number of free parameters can be reduced by assuming GUT unification with universal boundary conditions. Such a variant was thoroughly discussed in [6], so we do not repeat the full RGE analysis here. However its results can be qualitatively read also from the figures presented in this Section with the use of the following observations:

- (i) The neutron EDM is sensitive mostly to the masses of the first generation of squarks. Assuming universal sfermion masses at the GUT scale one can to a good approximation keep them degenerate also at  $M_Z$  scale. The remnant of the GUT evolution is their relation to the gaugino masses:  $m_Q^2 \approx m_D^2 \approx m_U^2 \approx m_0^2 + 6.5M_{1/2}^2 \approx m_0^2 + 10|M_2|^2$ , which leads to the relation  $m_Q \approx m_U \approx m_D \geq 3M_2$ .
- (ii) The  $\mu$  phase does not run. It is a free parameter anyway.
- (iii) The imaginary parts of the first generation  $A$  parameters,  $\text{Im}A_u$  and  $\text{Im}A_d$ , do not run, apart from the small corrections proportional to the Yukawa couplings of light fermions. Real parts of  $A_u$  and  $A_d$  run approximately in the same way. Hence universal boundary conditions at the GUT scale lead simply to  $\phi_{A_u} = \phi_{A_d}$  at the  $M_Z$  scale.
- (iv) RGE running suppresses the  $A_t$  phase (present in the CDM of gluons  $C_g$ ). Therefore, the low energy constraints are easy to satisfy even with large  $\phi_{A_t}$  at the GUT scale. The limits on  $\phi_{A_t}$  at the electroweak scale appear themselves to be rather weak.

- v) With universal gaugino masses and phases,  $M_1/\alpha_1 = M_2/\alpha_2 = M_3/\alpha_3$ , the common gaugino phase can be completely rotated away.

Using (i)–(v) one can use our plots for the universal GUT case, just assuming common  $A$  phase, neglecting  $\phi_{A_t}$  and looking at the part of plots for which  $m_Q \geq 3M_2$ . Again, in all figures of this Section we keep GUT related gaugino masses and degenerate squark mass parameters  $M_Q = M_D = M_U$ , so that the physical masses differ by D-terms only. We plot the results in terms of the physical mass of the  $D$ -squark  $m_D$ .

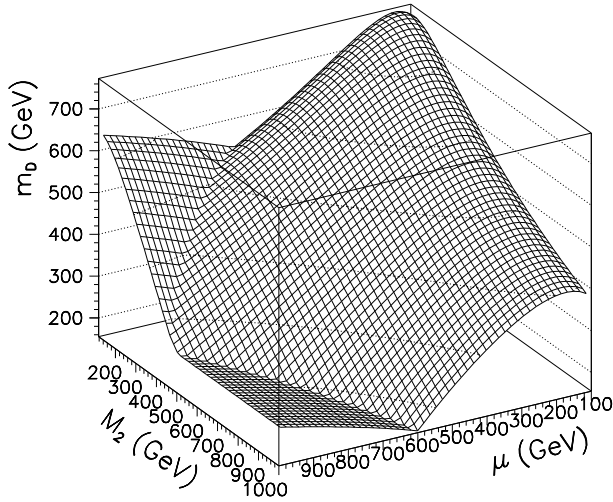


Fig. 9. Regions for which generic limits on  $|\sin \phi_\mu| \tan \beta$  given by neutron EDM are stronger then 0.05.

We consider first the limits on the  $\mu$  phase, neglecting the possibility of  $\mu - A$  cancellations. In Fig. 9 we show where the generic limits for the  $\mu$  phase given by the neutron EDM are strong. We plot there the area where the limit on  $|\sin \phi_\mu| \tan \beta$  given separately by the chargino, neutralino and gluino contributions to  $E_d$  and by the other contribution present in Eq.(15) summed up is stronger then 0.05. For small  $|\mu|$ ,  $|M_2|$ , squark masses  $m_Q \sim m_D \sim m_U > 750$  GeV are required to avoid the assumed limit.

The dominant contributions to the coefficient multiplying  $\sin \phi_\mu$  come from the first term of Eq. (15), *i.e.* from the d-quark EDM. The only exception is large  $|\mu|$  and light gauginos case, where also  $C_d$  becomes comparable to the other term. Both  $E_d, C_d$  are proportional to  $\mu \tan \beta$  so the  $\mu$  phase coefficient again scales approximately as  $\tan \beta$ . The largest contributions to  $\mu$  phase coefficient are given by the chargino and gluino (for small and large  $|\mu|$ , respectively) diagrams. They have the same sign, so, like in the electron case, the total  $\mu$  phase coefficient may disappear only if one allows

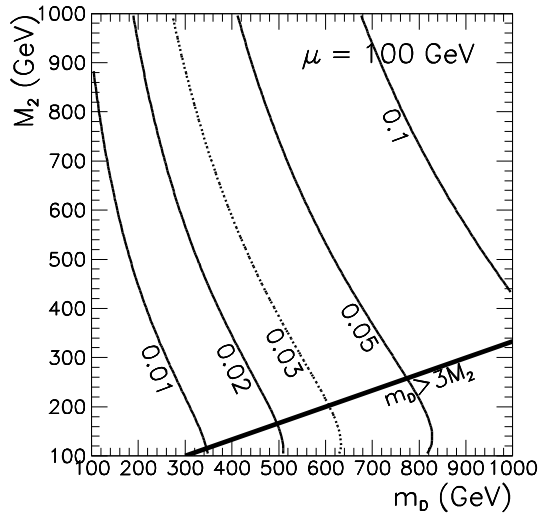


Fig. 10. Limits on  $|\sin \phi_\mu| \tan \beta$  given by the neutron EDM measurements.  $\phi_{A_u} = \phi_{A_d} = \phi_{A_t} = 0$  assumed.

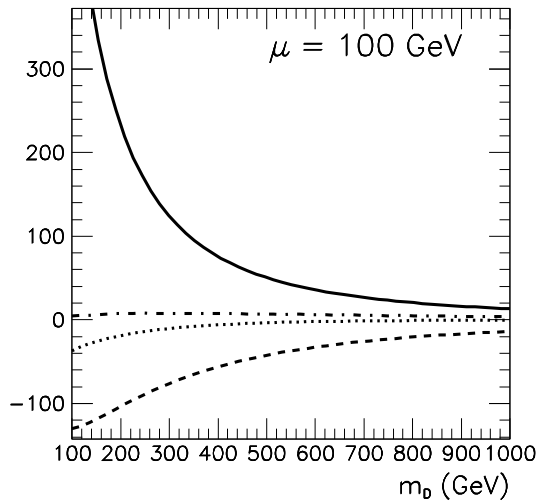


Fig. 11. Coefficients of  $\sin \phi_\mu \tan \beta$ ,  $|A_d|/m_D \sin \phi_{A_d}$ ,  $|A_u|/m_U \sin \phi_{A_u}$  and  $|A_t|/m_T \sin \phi_{A_t}$  terms in the neutron EDM (solid, dashed, dotted and dashed-dotted lines respectively).

the non-universal gaugino phases. The limits on  $|\sin \phi_\mu| \tan \beta$  on  $m_D - |M_2|$  plane are plotted in Fig. 10.

Some differences with the electron case may be observed in the structure of possible  $\mu - A$  cancellations. For  $E_e$  the term proportional to  $A_e$  orig-

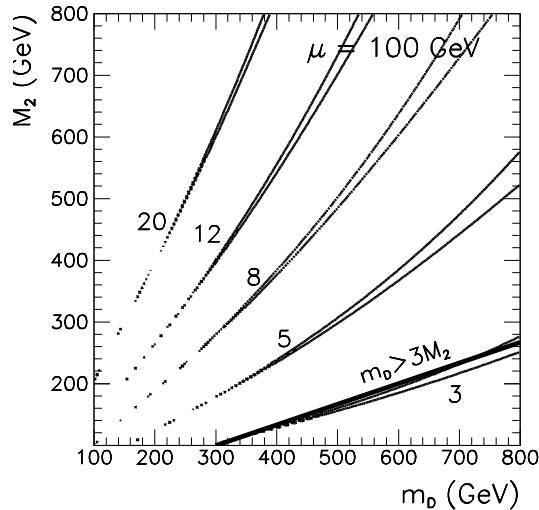


Fig. 12. Regions of  $m_D - |M_1|$  plane allowed by the neutron EDM measurement assuming  $\phi_\mu = \phi_{A_d} = \phi_{A_u} = \pi/2$ ,  $A_t = 0$  and various values of  $A_d/m_D = A_u/m_U$  (marked on the plots).

inates from the neutralino exchange diagram. For the neutron, additional contributions proportional to  $A_u$ ,  $A_d$  and  $A_t$  are given by the diagrams with gluino exchange and they have larger magnitude than those induced by neutralino loops, as illustrated in Fig. 11 (this effect is particularly strong for large  $|\mu|$  and light gauginos). This means that constraints on the  $A_I$  phases are somewhat stronger than in the electron case but, on the other hand, smaller  $A_I$  values are necessary for cancellations. For small  $|\mu| \sim 100$  GeV one needs  $A_e/m_E \geq 14$  but only  $A_d/m_D \sim A_u/m_U \geq 3$ . Furthermore, in unconstrained MSSM we have bigger freedom because of several different  $A_I$  parameters present in the formulae for  $E_n$ . Therefore, one has to take into account all  $A_I$  phases. In Fig. 12 we plot the regions of  $m_D - |M_1|$  plane allowed by the neutron EDM measurement assuming “maximal” CP violation  $\phi_\mu = \phi_{A_d} = \phi_{A_u} = \pi/2$  and various values of  $A_u/m_U = A_d/m_D$ .

The overall conclusion is that eventual cancellations in neutron EDM are more likely than in the electron case. They require somewhat smaller values of  $A$  parameters when one considers  $\mu - A$  phases cancellations. Assuming non-universal  $A_I$  parameters it is possible to suppress simultaneously both  $E_e$  and  $E_n$  values below the experimental constraints, at the cost of rather strong fine-tuning if the SUSY mass parameters are light.

#### 4. $\mu$ phase dependence of $\varepsilon_K$ , $\Delta m_B$ and $b \rightarrow s\gamma$

Analyzing the dependence of  $\bar{K}^0 K^0$  and  $\bar{B}B$  mixing on the SUSY phases, we assume again that there is no flavour violation in the squark mass matrices, so that only chargino and charged Higgs contributions to the matrix element do not vanish. Furthermore, only chargino exchange contribution depends on the  $\mu$ ,  $M_2$  and  $A$  phases and is interesting for our analysis. We consider the simplest case  $|\mu|, |M_2| \geq 2M_Z$ . In this case we can expand the matrix element in the mass insertion approximation:

$$(M_C)_{LLLL} \approx \left( K^\dagger Y_u^2 K \right)_{JI}^2 \left[ \frac{1}{8} D_2(|\mu|^2, |\mu|^2, m_U^2, m_U^2) + M_W^2 \text{Re}[(\mu^* \cos \beta + M_2 \sin \beta)(\mu \cos \beta + A_u^* \sin \beta)] \right. \\ \left. \times \frac{\partial}{\partial m_U^2} \frac{D_2(|\mu|^2, |\mu|^2, m_U^2, m_U^2) - D_2(|\mu|^2, |M_2|^2, m_U^2, m_U^2)}{|\mu|^2 - |M_2|^2} \right], \quad (16)$$

where one should put  $I = 2, J = 1$  for  $\bar{K}^0 K^0$  mixing,  $I = 3, J = 1$  for  $\bar{B}_d B_d$  mixing and  $I = 3, J = 2$  for  $\bar{B}_s B_s$  mixing (see [8] for the expression for loop function  $D_2$ ).  $\varepsilon_K$  and  $\Delta m_B$  are proportional, respectively, to the imaginary and real part of the matrix element. One can see immediately from the equation above that in the leading order it is sensitive only to  $|\mu|$  and to the real parts of the  $M_2\mu$ ,  $A_u\mu$  and  $M_2A_u^*$  products, *i.e.* to cosines of the appropriate phase combinations, not sins like the EDM's. Eventual effects of the phases can be thus visible only for large phase values. Even then, they are suppressed by the small numerical coefficient multiplying them. An example of the  $\varepsilon_K$  dependence on the  $\mu$  and  $A_u$  phases is presented in Fig. 13. As can be seen from the Figure, even for light SUSY particle masses the change of the  $\varepsilon_K$  value with variation of  $\mu$  and  $A$  phases is smaller than 5%.

In contrast to  $\varepsilon_K$  and  $\Delta m_B$ ,  $b \rightarrow s\gamma$  decay appears to depend strongly on the  $\mu$  (see Fig. 14) and  $A_t$  phases. The branching ratio  $\text{Br}(B \rightarrow X_s\gamma)$  depends, like in the  $\varepsilon_K$  case, on the real parts of the  $\mu$  and  $A_t$  parameters, *i.e.* on cosines of the phases. However, contrary to the  $\varepsilon_K$  case, this dependence is quite strong and growing with increase of  $\tan \beta$  and of the stop LR-mixing  $A_t$  parameter. Also, as follows from the discussion in the previous Section, the limits on  $A_t$  phase are rather weak, independently on  $\tan \beta$ , so one can expect large effects of this phase in  $\text{Br}(B \rightarrow X_s\gamma)$  decay.

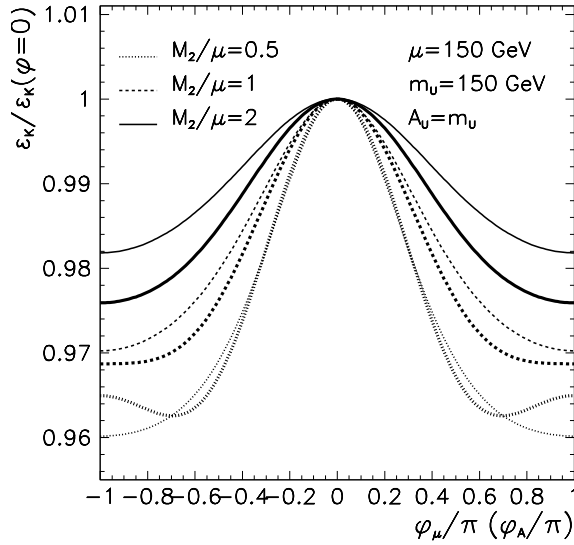


Fig. 13. Dependence of  $\varepsilon_K$  on  $\mu$  and  $A_u$  phases, normalized to  $\phi_\mu = \phi_{A_u} = 0$  case. Thin(thick) lines: dependence on  $\phi_\mu$  ( $\phi_{A_u}$ ) for  $\phi_{A_u}$  ( $\phi_\mu$ ) = 0.

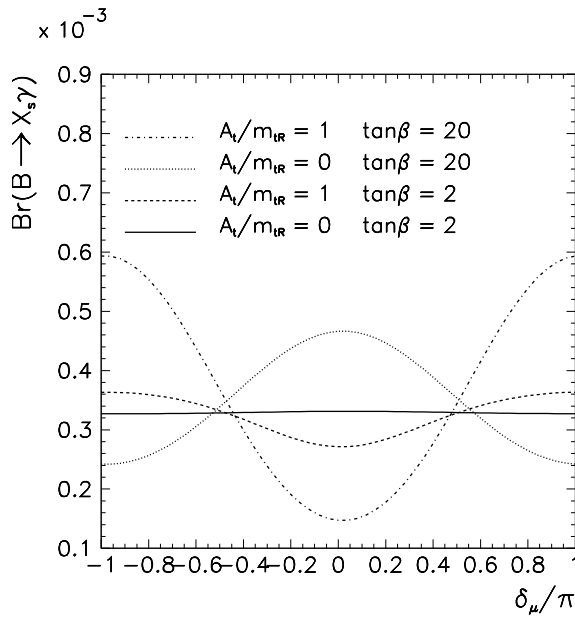


Fig. 14. Dependence of  $\text{Br}(B \rightarrow X_s \gamma)$  on  $\mu$  phase for  $m_A = 500$  GeV,  $|\mu| = |M_2| = \alpha_2/\alpha_1 |M_1| = 200$  GeV,  $m_{\tilde{t}_L} = 300$  GeV,  $m_{\tilde{t}_R} = 100$  GeV.

## 5. KM phase determination in MSSM

Because of the weak dependence of  $\varepsilon_K$  and  $\Delta m_B$  on flavour conserving supersymmetric CP phases, the determination of the KM matrix phase  $\delta_{\text{KM}}$  is basically unaffected by their eventual presence. However, even assuming no supersymmetric sources of CP violation at all, MSSM predictions for  $\bar{K}^0 K^0$  and  $\bar{B} B$  mixing are different from the SM one because the potentially significant contribution to CP violating transitions may come [16] from the (charged Higgs)-top and chargino-stop loops with Yukawa couplings and KM angles and phase in the vertices<sup>2</sup>. Since, in addition, several arguments based on GUT theories suggest that charginos and 3rd generation of sfermions may be among the lightest superpartners, it is interesting to discuss in more detail their impact on CP violation in SUSY models.

The present section is devoted to discussing such a scenario. The only extra MSSM contributions to the CP violating processes we consider are the (charged Higgs)-top and chargino-stop loops. Our results depend then on (apart from the SM parameters)  $\tan\beta$ , physical masses of the lighter and heavier stop ( $m_{\tilde{T}_1}$  and  $m_{\tilde{T}_2}$ , respectively), their mixing angle  $\theta_{LR}$ , chargino mass and mixing parameters - lightest chargino mass  $m_{\chi_1^\pm}$  and the ratio  $M_2/\mu$  and on the charged Higgs boson mass  $m_{H^\pm}$ .

In the considered approach to the MSSM,  $\Delta m_{B_d}$  and  $\varepsilon_K$  read as [19]:

$$\Delta m_{B_d} = \eta_{QCD} \frac{\alpha_{em}^2 m_t^2}{12 \sin^4 \theta_W M_W^4} f_{B_d}^2 B_{B_d} m_{B_d} |K_{tb} K_{td}^*|^2 |\Delta|, \quad (17)$$

$$|\varepsilon_K| = \frac{\sqrt{2} \alpha_{em}^2 m_c^2}{48 \sin^4 \theta_W M_W^4} f_K^2 B_K \frac{m_K}{\Delta m_K} |\mathcal{I} m \Omega|, \quad (18)$$

where

$$\begin{aligned} \Omega = & \eta_{cc} (K_{cs} K_{cd}^*)^2 + 2\eta_{ct} (K_{cs} K_{cd}^* K_{ts} K_{td}^*) f \left( \frac{m_c^2}{M_W^2}, \frac{m_t^2}{M_W^2} \right) \\ & + \eta_{tt} (K_{ts} K_{td}^*)^2 \frac{m_t^2}{m_c^2} \Delta, \end{aligned} \quad (19)$$

The charged Higgs and the chargino boxes enter, together with the SM terms, only into the quantity  $\Delta$  in the above equations (SM loops only give  $\Delta_{SM} \approx 0.53$ ). The QCD correction factors  $\eta_{xy}$  and  $\eta_{QCD}$  are given in [20].

---

<sup>2</sup> Chargino-sbottom loops could be important in  $\bar{D}^0 D^0$  mixing in large  $\tan\beta$  scenario. We do not consider here this possibility.

The KM elements appearing in Eqs. (17)–(19) can be conveniently expressed in terms of the Wolfenstein parameters  $\lambda$ ,  $A$ ,  $\rho$  and  $\eta$  [21]

$$K \approx \begin{pmatrix} 1 - \frac{\lambda^2}{2} & \lambda & A\lambda^3(\rho - i\eta) \\ -\lambda - iA^2\lambda^5\eta & 1 - \frac{\lambda^2}{2} + i\mathcal{O}(\lambda^6) & A\lambda^2 \\ A\lambda^3(1 - \rho - i\eta) & -A\lambda^2 - iA\lambda^4\eta & 1 \end{pmatrix} + \mathcal{O}(\lambda^4), \quad (20)$$

where  $\lambda = 0.22$  is known from semileptonic kaon and hyperon decays.

The theoretical predictions for  $\varepsilon_K$  and  $\Delta m_{B_d}$  have some uncertainty due to non-perturbative parameters  $B_K$ ,  $f_{B_d}^2 B_{B_d}$  which are known from lattice calculations, but not very precisely. Moreover, the KM element  $K_{td} = A\lambda^3(1 - \rho - i\eta)$  which appears in Eqs. (17)–(19) is not directly measured. Its SM value fitted to the observables in Eqs. (17)–(18) can change after inclusion of new contributions. Thus, the correct approach is to fit the parameters  $A$ ,  $\rho$ ,  $\eta$  and  $\Delta$  in a model independent way to the experimental values of  $\varepsilon_K$  and  $\Delta m_{B_d}$  [19]. The quantities  $|K_{cb}|$  and  $|K_{ub}/K_{cb}|$  are known from tree level processes. They are practically unaffected by new physics which contributes only at one and more loops.

Here, we give the results of such a fit, with  $B_K$  and  $f_{B_d}^2 B_{B_d}$  varied in a the following ranges: [18]:  $0.6 < B_K < 0.9$  and  $0.160 \text{ GeV} < \sqrt{f_{B_d}^2 B_{B_d}} < 0.240 \text{ GeV}$ . In our fit, we use the following experimental results [18]:

$$|K_{cb}| = 0.039 \pm 0.002, \quad (21)$$

$$|K_{ub}/K_{cb}| = 0.08 \pm 0.02, \quad (22)$$

$$|\varepsilon_K| = (2.26 \pm 0.02) 10^{-3}, \quad (23)$$

$$\Delta m_{B_d} = (3.01 \pm 0.13) 10^{-13} \text{ GeV}. \quad (24)$$

Scanning over allowed range for  $B_K$  and  $f_{B_d}(B_{B_d})^{1/2}$ , gives the “absolute” bounds<sup>3</sup> on  $\Delta$ . Such bounds are not very tight. After including  $1\sigma$  errors on  $\Delta$ , they are roughly

$$0.2 \lesssim \Delta \lesssim 2.0. \quad (25)$$

In Fig. 15, we plot the allowed ranges of  $\rho$  and  $\eta$  for several fixed values of  $\Delta = \frac{1}{2}\Delta_{SM}, \Delta_{SM}, 2\Delta_{SM}, 3\Delta_{SM}$  and changing  $B_K$ ,  $f_{B_d}(B_{B_d})^{1/2}$  in the ranges specified above. The allowed half-ring visible in the plots of Fig. 15 originates from  $|K_{ub}/K_{cb}|$  given in Eq. (22). The measurement of  $\Delta m_{B_d}$  allows another ring in the  $(\rho, \eta)$  plane. Its interesting part is approximately parallel to the  $\eta$  axis and moves towards larger  $\rho$  when  $\Delta$  increases.

<sup>3</sup> We assume that  $\Delta$  is real. This is true in the SM and in the considered approach to the MSSM. However, in a general MSSM,  $\Delta$  could develop a sizable imaginary part.

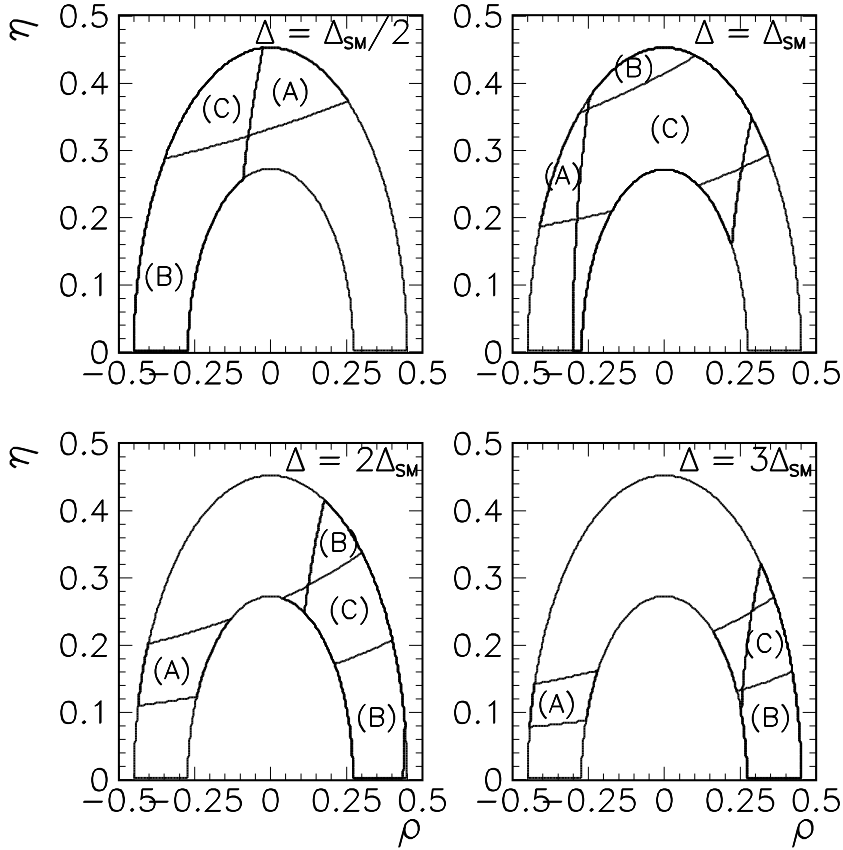


Fig. 15. Allowed regions in the  $(\rho, \eta)$  plane for four values of  $\Delta$ : (A) - allowed by  $\varepsilon_K$ , (B) - allowed by  $\Delta m_{B_d}$ , (C) - allowed by  $\varepsilon_K$  and  $\Delta m_{B_d}$ .

The range bounded by  $\varepsilon_K$  is approximately parallel to the  $\rho$  axis. It moves towards smaller  $\eta$  with increasing  $\Delta$ . Taking both effects into account, we can see that small  $\Delta$  prefers negative  $\rho$  and large  $\eta$ ,  $\Delta \sim \Delta_{SM}$  gives the biggest allowed range for  $\rho$  and  $\eta$  with both  $\rho < 0$  and  $\rho > 0$  possible, whereas larger  $\Delta \geq 1$  requires positive  $\rho$  and smaller  $\eta$ .

Theoretical analysis shows that in considered here scenario the values of  $\Delta$  in the MSSM are always bigger than in the SM, *i.e.* the new contributions to  $\Delta$  from the Higgs and chargino sectors have the same sign as  $\Delta_{SM}$ . The charged Higgs contribution increases  $\Delta$  by at most about 0.15 for light  $m_{H^\pm} = 100$ . The value of the chargino-stop contribution to  $\Delta$  depends strongly on the ratio  $M_2/\mu$ . For small values of  $|M_2/\mu|$ , when the lighter chargino is predominantly gaugino, it is very small (of order  $10^{-2}$ ). It grows with increasing  $|M_2/\mu|$ , when lighter chargino consists predominantly of

Higgsino, up to  $0.5 - 0.7$  for some parameter choices. In general, MSSM predicts  $\Delta$  in the range  $0.5 - 1.5$ . Comparing with the experimental fit to  $\Delta$  illustrated in Fig. 15, one can see that even in the complete absence of genuinely supersymmetric sources of CP violation, MSSM may give for the KM phase  $\delta_{\text{KM}}$  significantly different from the SM one.

## 6. Conclusions

We have reanalyzed the constraints on the phases of flavour conserving supersymmetric couplings that follow from the electron and neutron EDM measurements. We find that the constraints on the phases (particularly on the phase of  $\mu$ ) are generically strong  $\phi \leq 10^{-2}$  if all relevant supersymmetric masses are light, say  $\leq \mathcal{O}(500 \text{ GeV})$ . However, we also find that the constraints disappear or are substantially relaxed if just one of those masses, *e.g.* slepton mass, is large,  $m_E > \mathcal{O}(1 \text{ TeV})$ . Thus, the phases can be large even if some masses, *e.g.* the chargino masses, are small.

In the parameter range where the constraints are generically strong, there exist fine-tuned regions where cancellations between different contributions to the EDM can occur even for large phases. However, such cancellations have no obvious underlying symmetry principle. From the low energy point of view they look purely accidental and require not only  $\mu - A$ ,  $\mu - M_{\text{gaugino}}$  or  $M_1 - M_2$  phase adjustment but also strongly correlated with the phases and among themselves values of soft mass parameters. Therefore, with all soft masses, say  $\leq \mathcal{O}(1 \text{ TeV})$ , models with small phases look like the easiest solution to the experimental EDM constraints. This conclusion becomes stronger the higher is the value of  $\tan \beta$ , as the constraints on  $\mu$  phase scale as  $1/\tan \beta$ . Nevertheless, since the notion of fine tuning is not precise, particularly from the point of view of GUT models, it is not totally inconceivable that the rationale for large cancellations exists in the large energy scale physics. Therefore all experimental bounds on the supersymmetric parameters, and particularly on the Higgs boson masses [17], should include the possibility of large phases even if with large cancellations, to claim full model independence.

The dependence of  $\varepsilon_K$  and  $\Delta m_B$  on the supersymmetric phases is weak and gives no clue about their values. The  $\delta_{\text{KM}}$  determination remains essentially unaffected by the presence of SUSY phases but its value may change significantly (comparing to value fitted in SM) due to new charged Higgs and chargino contributions, depending on the real masses and mixing parameters. Large effects of SUSY phases may be observed in  $b \rightarrow s\gamma$  decay, but, apart from the  $\phi_\mu$  and  $\phi_{A_t}$  phases,  $b \rightarrow s\gamma$  amplitude depends on many free mass parameters, so it does not produce limits on the phases alone.

## REFERENCES

- [1] E. Commins *et al.*, *Phys. Rev.* **A50**, 2960 (1994); K. Abdullah *et al.*, *Phys. Rev. Lett.* **65**, 234 (1990).
- [2] P. G. Harris *et al.*, *Phys. Rev. Lett.* **82**, 904 (1999).
- [3] J. Ellis, S. Ferrara, D.V. Nanopoulos, *Phys. Lett.* **114B**, 231 (1982); W. Buchmüller, D. Wyler, *Phys. Lett.* **121B**, 321 (1983); J. Polchinski, M.B. Wise *Phys. Lett.* **125B**, 393 (1983).
- [4] P. Nath, *Phys. Rev. Lett.* **66**, 2565 (1991); Y. Kizuruki, N. Oshimo, *Phys. Rev.* **D45**, 1806 (1992); *Phys. Rev.* **D46**, 3025 (1992); R. Garisto, *Nucl. Phys.* **B419**, 279 (1994).
- [5] T. Falk, K.A. Olive *Phys. Lett.* **B439**, 71 (1998); *Phys. Lett.* **B375**, 196 (1996).
- [6] T. Ibrahim, P. Nath, *Phys. Lett.* **B418**, 98 (1998); *Phys. Rev.* **D57**, 478 (1998); *Phys. Rev.* **D58**, 111301 (1998); A. Bartl *et al.*, hep-ph/9903402.
- [7] M. Brhlik, G.J. Good, G.L. Kane, *Phys. Rev.* **D59**, 115004 (1999).
- [8] S. Pokorski, J. Rosiek, C. Savoy, hep-ph/9906206.
- [9] M. Dugan, B. Grinstein, L. Hall, *Nucl. Phys.* **B255**, 413 (1985).
- [10] J. Rosiek, *Phys. Rev.* **D41**, 3464 (1990), erratum hep-ph/9511250.
- [11] F. Gabbiani, E. Gabrielli, A. Masiero, L. Silvestrini, *Nucl. Phys.* **B477**, 321 (1996).
- [12] A. Manohar, H. Georgi, *Nucl. Phys.* **B234**, 189 (1984).
- [13] R. Arnowitt, J. Lopez, D.V. Nanopoulos *Phys. Rev.* **D42**, 2423 (1990); R. Arnowitt, M. Duff, K. Stelle, *Phys. Rev.* **D43**, 3085 (1991).
- [14] S. Weinberg, *Phys. Rev. Lett.* **63**, 2333 (1989); E. Braaten, C.S. Li, T.C. Yuan, *Phys. Rev. Lett.* **64**, 1709 (1990).
- [15] D. Chang, W.Y. Keung, A. Pilaftsis, *Phys. Rev. Lett.* **82**, 900 (1999).
- [16] M. Misiak, J. Rosiek, S. Pokorski, hep-ph/9703442, published in A. Buras, M. Lindner (eds.), *Heavy flavours II*, pp. 795-828, World Scientific Co.
- [17] A. Pilaftsis, C.E. Wagner, hep-ph/9902371.
- [18] A.J. Buras, hep-ph/9610461 and references therein.
- [19] A. Brignole, F. Feruglio, F. Zwirner, *Z. Phys.* **C71**, 679 (1996).
- [20] A.J. Buras, M. Jamin and P.H. Weisz, *Nucl. Phys.* **B347**, 491 (1990); S. Herlich, U. Nierste, *Nucl. Phys.* **B419**, 292 (1994), *Phys. Rev.* **D52**, 6505 (1995).
- [21] L. Wolfenstein, *Phys. Rev. Lett.* **51**, 1945 (1983).